1521-009X/44/8/1372–1380$25.00
Drug Metabolism and Disposition
http://dx.doi.org/10.1124/dmd.116.070409
Drug Metab Dispos 44:1372–1380, August 2016

Application of Static Models to Predict Midazolam Clinical Interactions in the Presence of Single or Multiple Hepatitis C Virus Drugs[S]

Yaofeng Cheng, Li Ma, Shu-Ying Chang, W. Griffith Humphreys, and Wenying Li

Pharmaceutical Candidate Optimization, Research and Development, Bristol-Myers Squibb, Princeton, New Jersey

Received March 10, 2016; accepted May 24, 2016

ABSTRACT

Asunaprevir (ASV), daclatasvir (DCV), and beclabuvir (BCV) are three drugs developed for the treatment of chronic hepatitis C virus infection. Here, we evaluated the CYP3A4 induction potential of each drug, as well as BCV-M1 (the major metabolite of BCV), in human hepatocytes by measuring CYP3A4 mRNA alteration. The induction responses were quantified as induction fold (mRNA fold change) and induction increase (mRNA fold increase), and then fitted with four nonlinear regression algorithms. Reversible inhibition and time-dependent inhibition (TDI) on CYP3A4 activity were determined to predict net drug-drug interactions (DDIs). All four compounds were CYP3A4 inducers and inhibitors, with ASV demonstrating TDI. The curve-fitting results demonstrated that fold increase is a better assessment to determine kinetic parameters for compounds inducing weak responses. By summing the contribution of each inducer, the basic static model was able to correctly predict the potential for a clinically meaningful induction signal for single or multiple perpetrators, but with over prediction of the magnitude. With the same approach, the mechanistic static model improved the prediction accuracy of DCV and BCV when including both induction and inhibition effects, but incorrectly predicted the net DDI effects for ASV alone or triple combinations. The predictions of ASV or the triple combination could be improved by only including the induction and reversible inhibition but not the ASV CYP3A4 TDI component. Those results demonstrated that static models can be applied as a tool to help project the DDI risk of multiple perpetrators using in vitro data.

Introduction

The study of cytochrome P450 (P450) enzyme induction has important clinical significance for drug development. According to the U.S. Food and Drug Administration (FDA) guidance for industry, one of the major objectives in evaluating in vitro drug metabolism is to explore the effects of the new chemical entity on the metabolism of other drugs and the effects of other drugs on its metabolism (FDA draft guidance, http://www.fda.gov/Drugs/GuidanceComplianceRegulatoryInformation/Guidances/default.htm). Induction of P450 enzymes may lead to reduced efficacy or adverse drug interactions by increasing the metabolism of other drugs that are substrates for the induced enzymes (Jana and Paliwal, 2007). Therefore, it is important to determine whether a drug candidate has the potential to interact with P450 enzymes. If this determination can be made in discovery or early development, the data can aid in more efficient clinical trial design. In addition, a negative result from in vitro experiments may preclude or reduce the need to perform corresponding in vivo clinical drug interaction studies.

Human microsomes are commonly used to investigate the inhibitory effect of drug candidates in vitro since the P450 activities are well maintained in those systems. However, P450 induction is mainly through the bindings of drugs to nuclear receptors that then guide the protein expression of a specific enzyme. For example, the induction of CYP3A4, CYP2B6, and CYP1A1 are through the activation of upstream transcription factors including the pregnane X receptor, constitutive androstane receptor, and aryl hydrocarbon receptor (Tompkins and Wallace, 2007). Therefore, the in vitro induction experiments are usually conducted in living cells, mostly in hepatocytes. Evaluation of CYP1A2, CYP2B6, and CYP3A mRNA induction in primary human hepatocytes are recommended with the generation of the maximal effect (E_{max}) and concentration at 50% of maximal effect (EC_{50}) values, which can then be used in model-based analysis to determine the potential for an in vivo signal and the need for further clinical evaluation.

Asunaprevir [(ASV) BMS-650032], daclatasvir [(DCV) BMS-790052], and beclabuvir [(BCV) BMS-791325] are three drugs developed for chronic hepatitis C virus (HCV) infection. ASV is a potent and selective inhibitor of HCV NS3 protease, with activity against genotypes 1 and 4 (McPhee et al., 2012). DCV is a highly selective HCV NS5A replication complex inhibitor with picomolar potency and antiviral activity against HCV genotypes 1–6 in vitro (Gao et al., 2010). BCV is a selective, nonnucleoside NS5B polymerase inhibitor (Gentles et al., 2014). These new generation HCV drugs have fewer complications when compared with conventional treatments consisting of a combination of antiviral drug(s) (i.e., ribavirin) and pegylated interferon (Wilkins et al., 2010). The DCV and ASV dual regimen has been approved in Japan and several nations across the Asia Pacific, Latin America, and Eastern Europe for patients with genotype 1 chronic HCV infection, and DCV has been approved in the United States, Europe, and Japan, and in multiple nations across Latin America, Middle East, and

dx.doi.org/10.1124/dmd.116.070409.
[S]This article has supplemental material available at dmd.aspetjournals.org.

ABBREVIATIONS: AIC_c, corrected Akaike information criterion; ASV, asunaprevir; AUCR, area under the curve ratio; BCV, beclabuvir; DCV, daclatasvir; DDI, drug-drug interaction; EC_{50}, concentration at 50% of maximal effect; E_{max}, maximal effect; FDA, Food and Drug Administration; HCV, hepatitis C virus; IC_{50}, concentration at 50% inhibition; LDH, lactate dehydrogenase; P450, cytochrome P450; TDI, time-dependent inhibition.

Asia Pacific for use in combination with other medicines for HCV genotypes 1, 2, 3, and 4. The triple combination of DCV, ASV, and BCV is under regulatory review.

Following an oral dose, metabolites contribute less than 10% of the drug-related systemic exposure in humans for both ASV and DCV (Eley et al., 2013; Gong et al., 2016). A major metabolite of BCV, BCV-M1, was observed in humans, up to 24.6% of total exposure in plasma (Sims et al., 2014). Based on FDA draft guidance (http://www.fda.gov/Drugs/GuidanceComplianceRegulatoryInformation/Guidances/default.htm), metabolites found at greater than 10% of parent drug systemic exposure at steady state in human plasma can raise a safety concern and should be characterized. The 10% threshold was further clarified, and a major metabolite has been defined as a human metabolite that comprises greater than 10% of the measured total exposure to drug and metabolites (FDA draft guidance, http://www.fda.gov/Drugs/GuidanceComplianceRegulatoryInformation/Guidances/default.htm). Therefore, BCV-M1, but no other metabolite of these HCV drugs, was characterized in nonclinical studies, including in vitro P450 inhibition and induction evaluations. Since inhibition assays were conducted following well-established methods (Yao et al., 2007; Chang et al., 2010) with minor changes, the results of those studies are presented without inclusion of experimental methods. Here, we describe our experience and rationale for conduction of induction studies, including experimental design, selection of data sets, and nonlinear regression algorithms for curve fitting to determine the induction E_{max} and EC_{50} values, and we provide a structured approach for data processing. In addition, we explored the possibility of using basic and mechanistic static models to predict the in vivo drug-drug interaction (DDI) risk in the presence of multiple perpetrators.

Materials and Methods

Chemicals. ASV (BMS-650032), DCV (BMS-790052), BCV (BMS-791325), and BCV-M1 (a major metabolite of BCV) were synthesized at Bristol-Myers Squibb Co. (New Brunswick, NJ) (Gao et al., 2010; Gentles et al., 2014; Scola et al., 2014). Their structures are shown in Fig. 1. Rifampin was purchased from Sigma (St. Louis, MO). All other reagents and solvents were of analytical grade.

CYP3A4 Induction in Human Hepatocytes. The criteria to select compound concentrations were based on the clinical maximum plasma concentration (C_{max}) at steady state and the highest concentration that did not cause cytotoxicity evaluated by lactate dehydrogenase (LDH) release. Concentrations of each test compound were as follows: ASV (0.049, 0.15, 0.49, 1, 2, 4.9, 10, and 20 μg/ml); DCV (0.16, 0.32, 0.75, 1.6, 2.5, 4, 6, and 9.6 μg/ml); BCV (0.15, 0.35, 0.8, 1.5, 3.5, 8, 15, and 30 μg/ml); and BCV-M1 (0.028, 0.08, 0.28, 0.8, 2.8, 8, 15, and 30 μg/ml). The P450 induction experiments were conducted by XenoTech LLC (Lenexa, KS) using sandwich cultured cryopreserved hepatocytes from three male donors according to XenoTech's protocol and previously described methods (Robertson et al., 2000; Madan et al., 2003; Paris et al., 2009). Each compound was tested with three different lots of hepatocytes. Hepatocyte lots HC3-15, HC5-10, and HC1-18 were used to evaluate ASV and DCV, while hepatocyte lots HC3-15, HC5-10, and HC3-17 were used to evaluate BCV and BCV-M1. The hepatocyte cultures were treated for three consecutive days with 0.1% v/v dimethylsulfoxide (vehicle control), Bristol-Myers Squibb compounds, or rifampin (10 μM, positive control). Cytotoxicity was assessed by visual inspection of cell morphology and by measuring LDH activity in the incubation media with the Cytotoxicity Detection Kit (Roche Diagnostics Co., Indianapolis, IN). Approximately 24 hours following the last treatment, media were removed. The cells were washed with fresh culture media and total RNA was isolated from the cells using TRIzol RNA Isolation Reagent (Life Technologies, Grand Island, NY) and purified using the RNAeasy Mini Kit (Qiagen Inc. Gaithsburg, MD), according to the manufacturers' instructions. Single-stranded cDNA preparation and quantitative reverse-transcription polymerase chain reaction were performed using the AB 7900HT Fast Real Time PCR System (Applied Biosystems, Foster City, CA), following the Applied Biosystems protocol. The quantitative reverse-transcription polymerase chain reaction data were processed using the Sequence Detection System (software version 1.4 or 2.3), for relative quantification (Applied Biosystems). The target gene (CYP3A4) signals were normalized to the endogenous gene control (glyceraldehyde 3-phosphate dehydrogenase) as follows:

$$\Delta C_t = C_t(\text{CYP3A4}) - C_t(\text{glyceraldehyde 3 - phosphate dehydrogenase}). \quad (1)$$

Relative gene expression was obtained by comparing the normalized target gene signal in the compound-treated sample to the vehicle control (eq. 2), which is defined as "fold induction" in this paper. Fold increase is the change in gene expression, which is calculated in eq. 3.

$$\text{fold induction} = 2 - [\Delta C_t(\text{test compound}) - \Delta C_t(\text{vehicle compound})] \quad (2)$$

$$\text{fold increase} = \text{fold induction} - 1 \quad (3)$$

In vitro Induction Model Fitting. The maximum induction response (E_{max}) and concentration causing half-E_{max} (EC_{50}) were calculated based on both fold induction and fold increase data. For the purpose of curve fitting, data points were excluded from the fitting if they had concentrations greater than the one causing the highest response (observed E_{max}) but had measured mRNA levels that were less than 80% of the observed E_{max}. Induction responses were fit using the following four nonlinear regression algorithms (model) using GraphPad Prism, version 5 (GraphPad Software, Inc., La Jolla, CA) or Sigma Plot V12 (Systat Software, Inc., San Jose, CA):

Simple E_{max} model

$$E = \frac{E_{max} \times C}{EC_{50} + C} \quad (4)$$

Sigmoid Hill model

$$E = \frac{E_{max} \times C^H}{EC_{50}{}^H + C^H} \quad (5)$$

Sigmoid 3 parameter model

$$E = \frac{E_{max}}{1 + e^{(EC_{50} - C)/H}} \quad (6)$$

Four parameter logic model

$$E = D + \frac{E_{max} - D}{1 + (EC_{50}/C)^H} \quad (7)$$

where E is the observed induction effect in the presence of inducer at different concentrations (C); and D denotes the induction effect after treatment with the dimethylsulfoxide vehicle. The best-fit model was selected based on the lowest corrected Akaike information criterion (AIC_c), which was calculated with the following equation:

$$AIC_c = N \times \ln\frac{SS}{N} + \frac{2N \times P}{N - P - 1} \quad (8)$$

where N is the number of data points used in the fitting; SS is the residual sum of squares of the fitting; and P is the number of parameters in the fitting model (Sugiura, 1978).

CYP3A4 Inhibition Assays in Human Liver Microsomes. To predict the net DDI effect, the reversal inhibition and time-dependent inhibition (TDI) of ASV, DCV, BCV, and BCV-M1 on CYP3A4 were evaluated in human liver microsomes based on published methods (Yao et al., 2007; Chang et al., 2010). A brief description of the experiment procedures and data processing is available in the Supplemental Material. The concentration of midazolam in the assay (5 μM) was close to the K_M value of midazolam determined in the assay (4.13 μM) (Yao et al., 2007); therefore, the K_i value was estimated to be one-half of the IC_{50} value according to the Cheng-Prusoff equation (Cheng and Prusoff, 1973) by assuming that the test compound is a competitive inhibitor of CYP3A4. All incubations were run in triplicate and the mean values of the triplicates were used to calculate the inhibition parameters.

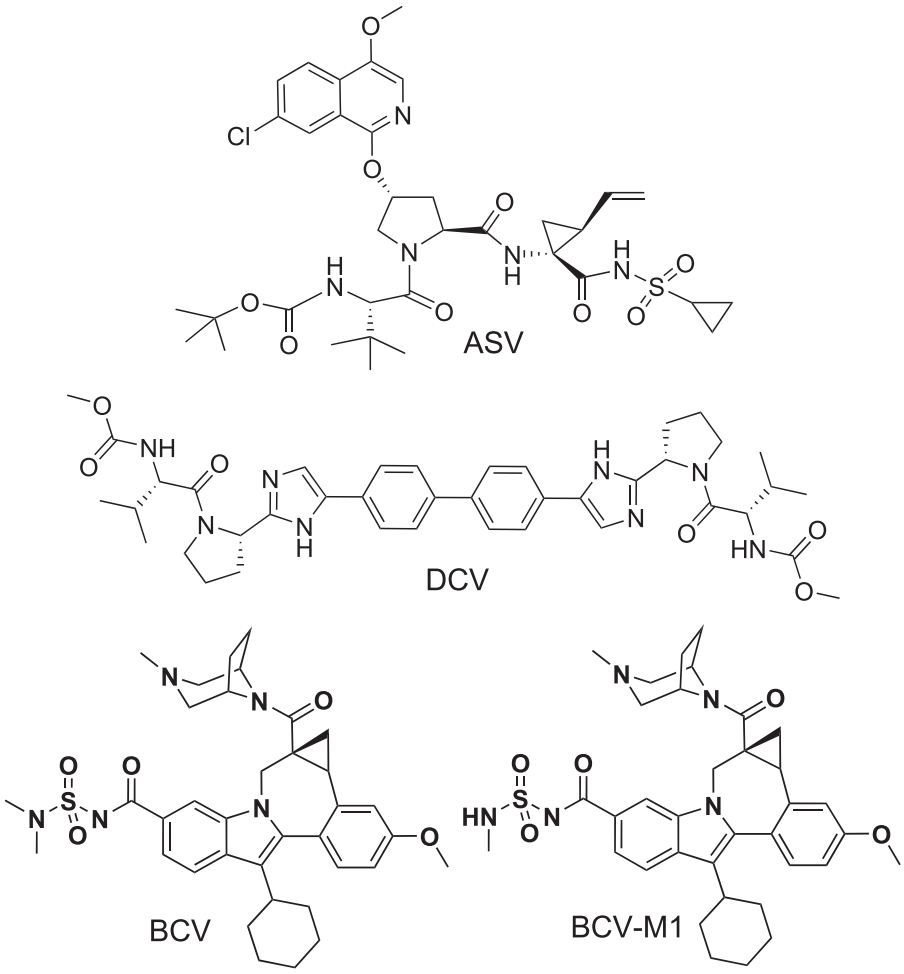

Fig. 1. Chemical structures of ASV (BMS-650032), DCV (BMS-790052), BCV (BMS-791325), and BCV-M1 (major metabolite of BCV).

In vivo Interaction Prediction. The in vivo DDI risk was predicted using the modified basic static model (R_3) and mechanistic static model [area under the curve ratio (AUCR)], as given by

$$R_3 = \frac{1}{1+\sum_{p=1}^{n}\left[\left(d\times E_{\max,p}\times [I]_p\right)\Big/\left([I]_p+\mathrm{EC}_{50,p}\right)\right]} \tag{9}$$

$$\mathrm{AUCR} = \frac{1}{f_m\times(A\times B\times C)+(1-f_m)}\times\frac{1}{(X\times Y\times Z)\times(1-F_G)+F_G} \tag{10}$$

where A, B, and C represent the reversible inhibition, TDI, and induction in liver, respectively; and X, Y, and Z represent the reversible inhibition, TDI, and induction in the gastrointestinal track, respectively. They are defined as

$$A = \frac{1}{1+\sum_{p=1}^{n}\left([I]_{H,p}\Big/K_{i,u,p}\right)} \tag{10a}$$

$$B = \frac{k_{deg,H}}{k_{deg,H}+\sum_{p=1}^{n}\left[\left([I]_{H,p}\times k_{inact,p}\right)\Big/\left([I]_{H,p}+K_{I,u,p}\right)\right]} \tag{10b}$$

$$C = 1+\sum_{p=1}^{n}\frac{d\times E_{\max,p}\times [I]_{H,p}}{[I]_{H,p}+\mathrm{EC}_{50,p}} \tag{10c}$$

$$X = \frac{1}{1+\sum_{p=1}^{n}\left([I]_{G,p}\Big/K_{i,u,p}\right)} \tag{10d}$$

$$Y = \frac{k_{deg,G}}{k_{deg,G}+\sum_{p=1}^{n}\left[\left([I]_{G,p}\times k_{inact,p}\right)\Big/\left([I]_{G,p}+K_{I,u,p}\right)\right]} \tag{10e}$$

$$Z = 1+\sum_{p=1}^{n}\frac{d\times E_{\max,p}\times [I]_{G,p}}{[I]_{G,p}+\mathrm{EC}_{50,p}} \tag{10f}$$

where p is the number of perpetrators; and $[I]$ is the total plasma concentration. The degradation rates for CYP3A4 in the liver ($k_{deg,H}$) and intestine ($k_{deg,G}$) were 0.00032 and 0.00048 per minute (Fahmi et al., 2008, 2009). The fraction of the midazolam metabolized by CYP3A (f_m) and the fraction of midazolam escaping intestinal extraction (F_G) are 0.90 and 0.51, respectively (Obach et al., 2007). Here, $K_{i,u}$, K_{inact}, and $K_{I,u}$ represent the unbound reverse inhibition constant, maximum inactivation, and TDI constant, respectively; d represents a calibrator factor, and a value of 1 is used in both eqs. 9 and 10; and $[I]_H$ and $[I]_G$ represent the perpetrator-free portal vein concentration and gut enterocytes concentration, respectively, which are estimated by

$$[I]_H = f_u\times\left(C_{\max}+\frac{D\times K_a\times F_a}{Q_H\times \mathrm{BP}}\right) \tag{10g}$$

$$[I]_G = \frac{D\times K_a\times F_a}{Q_G} \tag{10h}$$

where D is the oral dose and f_u is the fraction of unbound drug in human serum. The values of hepatic blood flow (Q_H) and enterocytes blood flow (Q_G) used here are 1616 and 300 ml/min, respectively. The first-order absorption rate (K_a) was determined by first-order modeling fitting of the plasma concentration profile following an oral dose using Phoenix WinNonlin (Certara, L.P., Princeton, NJ). The human blood-to-plasma (BP) ratios for DCV, ASV, and BCV were determined to be 0.8, 0.55, and 0.7, respectively (unpublished data). Fraction of absorption (F_a) was derived from absolute bioavailability (F), and fraction of dose that escapes first-pass metabolism in gut (F_g) and liver (F_h) was derived using the equation $F = F_a\times F_g\times F_h$, in which F_g was assumed to be 1. Since hepatic

clearance is the major clearance pathway for DCV (DAKLINZA package insert, Bristol-Myers Squibb, Inc., Princeton, NJ; http://packageinserts.bms.com/pi/pi_daklinza.pdf), ASV (SUNVEPRA package insert, Bristol-Myers Squibb Australia Pty Ltd., Mulgrave, VIC, Australia; http://www.guildlink.com.au/gc/ws/bms/pi.cfm?product=bqpsunve10715), and BCV (unpublished data), the F_h value can be estimated based on $F_h = 1 - CL/(BP \times Q_H)$, in which CL is the plasma clearance. The F and CL values were obtained in clinical studies as 67% and 4.2 l/h for DCV (DAKLINZA package insert), 9.3% and 49.5 l/h for ASV (SUNVEPRA package insert), and 66.1% and 5.6 l/h for BCV (unpublished data).

To predict the in vivo induction effect in the presence of a single perpetrator, the R_3 values were calculated using either the average or individual values of EC_{50} and E_{max} or individual values from three different donors. In the case of the AUCR, the net DDI effects of ASV, DCV, and BCV were determined with the average inhibitor kinetic parameters together with the average or individual EC_{50} and E_{max} values. Since only two lots of hepatocytes (HC3-15 and HC5-10) were used to test the induction potential of all four compounds, the individual R_3 and AUCR values for combination treatments were only calculated in those two cases.

Results

The CYP3A4 mRNA induction data for ASV, DCV, BCV, and BCV-M1 are listed in Table 1. The positive control of the CYP3A4 inducer, rifampin, caused 3.7- to 29.8-fold induction compared with the dimethylsulfoxide vehicle control in three human donors, suggesting that the assay system functioned with adequate sensitivity. Upon treatment of cryopreserved human hepatocytes with test compounds, bell-shaped induction-concentration curves were observed for ASV, BCV, and BCV-M1. This may be caused by mild cytotoxicity effects at higher concentrations, even though it was not evidenced in the LDH release assay.

The induction response was fitted to four kinetic models as described in *Materials and Methods*. The E_{max} and EC_{50} values of each compound fitting using all four models are presented in Supplemental Table 2. The AIC_c values were calculated for each model, and the model with the lowest AIC_c value was selected to determine the induction kinetic parameters. Among the 24 model fittings, the simple E_{max} model was selected most frequently (15/24). The determined E_{max} and EC_{50} values are summarized in Table 2. BCV was the most potent inducer among the four compounds, followed by BCV-M1, ASV, and DCV.

For comparison, both the fold induction and fold increase of mRNA levels were fitted with the four kinetic models. Different outcomes with fold induction and fold increase were observed (Table 2). The differences may not be noticeable in the results with large induction response, but become significant with small induction response (up to 15-fold difference between fold induction and fold increase). As an example, curve fitting with the simple E_{max} model gave quite different EC_{50} values for fold induction and fold increase (Fig. 2). The difference was most significant for donor 2, in which the observed E_{max} value was small (Fig. 2C). While applying the four parameter logic model, the EC_{50} values were not different when fitting with fold induction and fold increase (Fig. 2D); however, since the four parameter logic model generated a larger AIC_c value, it was not selected for E_{max} and EC_{50} determination. With the corrected induction response (fold increase), an EC_{50} value of 0.45 μg/ml was determined (as shown in Fig. 2C), which is very close to the EC_{50} value of 0.36 μg/ml shown in Fig. 2D.

DCV, ASV, BCV, and BCV-M1 were also found to be inhibitors of CYP3A4 in human liver microsome incubations. The initial study found that the four drugs demonstrated increased potency to inhibit CYP3A4 with 30-minute preincubation (Supplemental Fig. 1; Supplemental Table 1). The IC_{50} values of DCV, BCV, and BCV-M1 were reduced approximately by half, but the IC_{50} value of ASV was decreased more than 5-fold. Thus, the TDI of ASV was further evaluated to determine TDI kinetics (Supplemental Figs. 2 and 3; Supplemental Table 1). The parameters for DDI predictions are listed in Table 3.

TABLE 1

CYP3A4 mRNA change relative to dimethylsulfoxide (DMSO) (0.1%) treatment in hepatocytes from three human donors following incubation with ASV, DCV, BCV, or BCV-M1

Drug	Treatment	CYP3A4 mRNA[a]		
		Donor 1	Donor 2	Donor 3
ASV	Donor	HC3-15	HC1-18	HC5-10
	DMSO (0.1%)	1	1	1
	0.049 μg/ml	3.73[b]	ND	0.802
	0.15 μg/ml	1.53	1.86	1.13
	0.49 μg/ml	4.72	3.58	1.77
	1 μg/ml	7.79	5.5	2.92
	2 μg/ml	8.6	ND	3.66
	4.9 μg/ml	12.1	6.7	4.3
	10 μg/ml	8.7[c]	4.73[c]	3.7
	20 μg/ml	4.95[c]	2.39[c]	1.74[c]
	Rifampin (10 μM)	26	18.1	8.15
DCV	Donor	HC3-15	HC1-18	HC5-10
	DMSO (0.1%)	1	1	1
	0.16 μg/ml	1.38	1.45	1.21
	0.32 μg/ml	1.44	1.66	1.34
	0.75 μg/ml	2.5	2.27	1.47
	1.6 μg/ml	5.59	5.7	4.91
	2.5 μg/ml	7.48	9.22	3.7
	4 μg/ml	12.8	12.1	6.35
	6 μg/ml	20.3	13.2	6.68
	9.6 μg/ml	27.3	13	8.76
	Rifampin (10 μM)	26	18.1	8.15
BCV	Donor	HC3-15	HC3-17	HC5-10
	DMSO (0.1%)	1.00	1.00	1.00
	0.15 μg/ml	1.96	1.45	1.90
	0.35 μg/ml	3.27	1.99	1.67
	0.8 μg/ml	5.64	2.59	2.67
	1.5 μg/ml	6.36	2.61	2.43
	3.5 μg/ml	5.77	2.18	2.64
	8 μg/ml	3.88[c]	2.09	2.45
	15 μg/ml	2.70[c]	1.38[c]	1.43[c]
	30 μg/ml	0.29[c]	0.08[c]	0.26[c]
	Rifampin (10 μM)	29.80	3.70	7.93
BCV-M1	Donor	HC3-15	HC3-17	HC5-10
	DMSO (0.1%)	1.00	1.00	1.00
	0.028 μg/ml	1.04	1.15	0.97
	0.08 μg/ml	1.63	1.26	1.05
	0.28 μg/ml	3.57	1.99	1.61
	0.8 μg/ml	7.17	2.49	2.22
	2.8 μg/ml	8.23	2.26	2.41
	8 μg/ml	5.24[c]	2.14	1.89[c]
	15 μg/ml	3.78[c]	1.87[c]	3.08
	30 μg/ml	0.32[c]	0.15[c]	0.14[c]
	Rifampin (10 μM)	29.80	3.70	7.93

ND, not determined due to sample analysis error.

[a]Values are relative to vehicle control, normalized to glyceraldehyde 3-phosphate dehydrogenase and are the average of triplicate determinations.

[b]Anomalous data, possibly due to sample analysis error. Data were excluded from the curve fitting.

[c]Data were excluded from the curve fitting because fold increase was <80% of the observed E_{max}value.

Several clinical studies were conducted to evaluate the effects of HCV drugs at different doses and combinations on the pharmacokinetics of midazolam. The study design, doses, and observed pharmacokinetic parameters are summarized in Table 4. The in vivo interaction effects were first estimated using the basic static model (R_3). In the treatment of ASV (200 and 600 mg) or DCV (60 mg), a single inducer was considered in the prediction. In the treatment of BCV (150 and 300 mg), Triple I, or Triple II, the R_3 values were calculated based on the effect of multiple inducers. Overall, the R_3 model can correctly predict the in vivo induction risk in both cases using either average or individual E_{max} and EC_{50} values. All seven treatments were predicted to cause the induction effect, which agrees with the clinical results (Table 5). However, the R_3 model overpredicted the induction potency for both single and multiple inducers.

TABLE 2

Induction kinetic parameters (E_{max} and EC_{50}) of ASV, DCV, BCV, and BCV-M1 following incubation with hepatocytes from three individual donors

Drug	Parameter	Fold Induction			Fold Increase		
		HC3-15	HC1-18/HC3-17[a]	HC5-10	HC3-15	HC1-18/HC3-17[a]	HC5-10
ASV	E_{max}	14.21	6.74	3.94	14.10	6.68	3.00
	EC_{50} (μg/ml)	1.00	0.61	0.58	1.38	0.68	0.78
DCV	E_{max}	28.24	13.05	8.27	45.30	11.90	12.80
	EC_{50} (μg/ml)	4.32	1.83	2.38	7.64	1.96	6.54
BCV	E_{max}	6.54	2.36	2.44	6.17	2.23	1.64
	EC_{50} (μg/ml)	0.20	0.03	0.02	0.46	0.45	0.19
BCV-M1	E_{max}	9.68	2.30	2.74	9.13	1.55	1.62
	EC_{50} (μg/ml)	0.39	0.02	0.21	0.58	0.19	0.47

[a]Induction of ASV and DCV was evaluated using lot HC1-18 hepatocytes; induction of BCV and BCV-M1 was evaluated using lot HC3-17 hepatocytes.

The net DDI effect of these perpetrators on midazolam exposure was also estimated using the mechanistic static model. When considering the induction together with inhibition, the mechanistic static model was able to correctly predict the interaction risk of DCV (60 mg every day) and BCV (150 and 300 mg twice a day). As shown in Table 5, the predicted AUCRs using average E_{max} and EC_{50} values are 0.43, 0.53, and 0.55 for the group of DCV (60 mg every day), BCV (150 mg twice a day), and BCV (300 mg twice a day), respectively. Additionally, the AUCR values are closer to the observed clinical area under the curve changes than the R_3 values. However, the mechanistic static model predicted net inhibition (AUCR $>$ 1) for the clinical studies with ASV and two triple combinations while considering induction, inhibition, and TDI. Those false predictions were corrected by not including the TDI component of ASV on CYP3A4 activity. This adjusted mechanistic static model (AUCR′) not only could predict the induction risk for ASV and triple combinations but also returned better results than the basic static model (R_3). Similar results were also observed when using the individual E_{max} and EC_{50} values to predict the net DDI effect.

Discussion

Hepatocytes are widely recognized as the most appropriate in vitro model to study the potential of new drugs to induce hepatic metabolism enzymes. Due to interspecies differences, primary cultures of human hepatocytes have become the system of choice over studies performed with animals. It has been shown that when human hepatocytes are overlaid with an extracellular matrix, such as Matrigel or collagen, the cells retain the ability to respond to prototypical P450 inducers (LeCluyse et al., 2000; LeCluyse, 2001). This straightforward screening method has been of great importance in drug development efforts, yielding both predictive and species-relevant data. To best determine the values of E_{max} and EC_{50} in human hepatocytes, 6–8 concentrations of

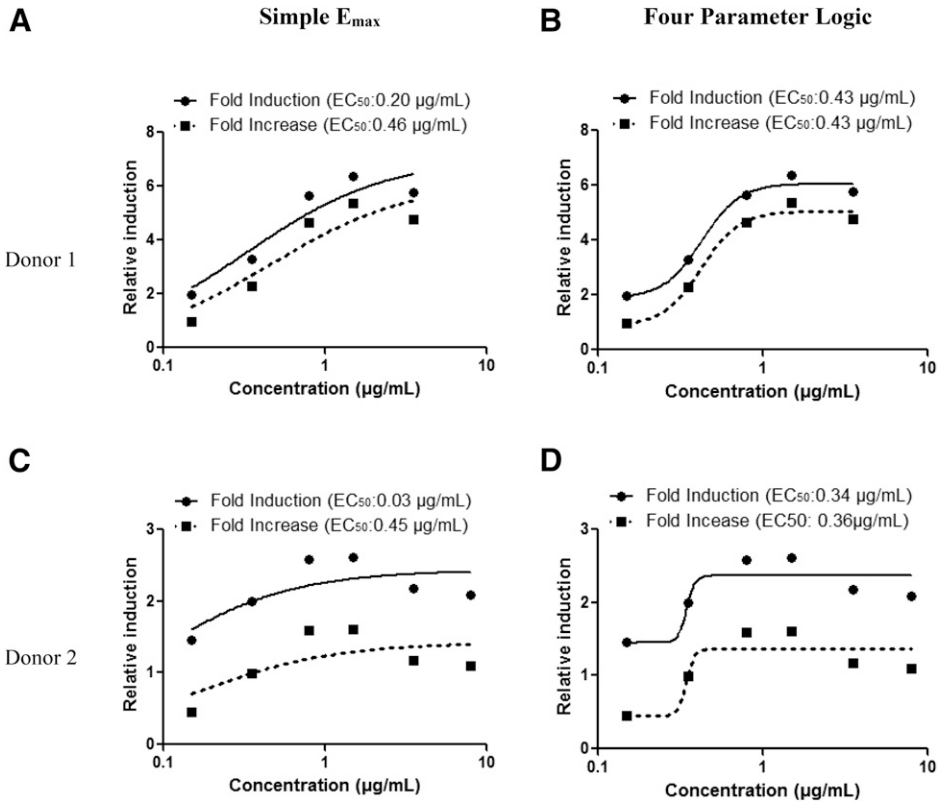

Fig. 2. Curve fitting of CYP3A4 mRNA induction data from two individual donor hepatocytes treated with BCV using the simple E_{max} model (A: donor 1; C: donor 2) and the four parameter logic model. (B: donor 1; D: donor 2)

TABLE 3

In vitro kinetic parameters of ASV, DCV, BCV, and BCV-M1 interaction with human CYP3A4

Drug	Reverse inhibition, $K_{i,u}$	TDI		Induction	
		K_{inact}	$K_{I,u}$	E_{max}	EC_{50}
	μg/ml	*1/min*	*μg/ml*		*μg/ml*
ASV	2.72	0.032	1.035	7.93	0.95
DCV	1.91	ND	ND	23.33	5.38
BCV	2.62	ND	ND	3.35	0.37
BCV-M1	1.95	ND	ND	4.10	0.41

ND, not determined

the test compound are recommended. In general, the lowest test concentration should be set close to one-tenth of the maximum plasma concentration (or projected maximum plasma concentration) in humans at a relevant clinical dose, while the top test concentration should go as high as possible to reach the induction response plateau, unless the response is limited by solubility or cytotoxicity. Despite the general consensus on basic experimental design, there remain some inconsistencies in data processing methods and a general lack of results on how to extrapolate in vitro induction data on single compounds to clinical situations involving mixtures of those compounds.

Four nonlinear regression algorithms—the simple E_{max}, sigmoid Hill, sigmoid 3 parameter, and four parameter logic models—have been suggested for curve fitting of in vitro induction data (Einolf et al., 2014). Induction studies often are designed with the number of test concentration levels set in order to collect a robust data set (as mentioned previously, eight concentrations), but also to conserve the number of hepatocytes used. The number of data points may become even smaller in the case of solubility or cytotoxicity issues, and for many compounds these factors can provide challenges to getting complete response values over the concentration range of interest. For the four compounds tested in our study, three seemed to cause mild cytotoxicity, evidenced by the decreased induction at higher concentration; however, cytotoxicity was not detected when measured by LDH release assay. These data points were excluded from the analysis, and thus the experiment produced a reduced number of data points for regression models. A model with a higher number of parameters tends to over-fit the induction data since it has more freedom to fit. Thus, the AIC_c value can be used to compare models and select the best fit model since it corrects sample size and is considered more accurate with small sample size (Sugiura, 1978). If $N \leq P$, the model should not be considered since it indicated that there are insufficient data points. If $N = P + 1$, the AIC_c value will not be calculable, but the model can be selected if other models fail. In addition, the AIC_c method penalizes extra parameters (P) for a fitting model, which is different from using standard error or R-squares as a way to select the best-fit model. Not surprisingly, with 4–7 available data points in our induction data set, the simple E_{max} model was selected in most of the cases to be the best-fit model over the other three models.

An aspect of data processing to determine induction parameters that is not entirely consistent in the literature is how to fit the no induction value when performing curve fitting. The value of fold induction has been used to calculate the E_{max} and EC_{50} values in many literature reports. The fold induction parameter would normally be set at 1 for the vehicle control. However, for the simple E_{max} and sigmoid Hill models the values should more appropriately be set at 0. To correct this discrepancy, we have used a parameter termed fold increase (as defined in *Materials and Methods*). While fitting with the fold induction value, the underestimation of EC_{50} values may not be noticeable for compounds with large induction responses; however, it can be significant for compounds with low induction response, as shown in Fig. 2. In addition, the E_{max} value determined using fold increase is more consistent with results from induction prediction models. For example, the E_{max} values for a

TABLE 4

Summary of clinical studies and pharmacokinetic parameters

Perpetrator Drug						Midazolam Oral Dose	Reference
Drug	Oral Dose	C_{max}	f_u	k_a	F_a		
	mg	*μg/ml*		*min*$^{-1}$		*mg*	
ASV (twice a day)	200	0.351	0.002	0.0063[a]	1[b]	5	Eley et al. (2011)
ASV (twice a day)	600	0.632	0.002	0.0053[a]	1[b]	5	Unpublished data[c]
DCV (every day)	60	1.288	0.006	0.013[a]	0.71	5	Bifano et al. (2013)
BCV (twice a day)	150	1.835[d]/0.434[e]	0.012[d,e]	0.0067[a,d]	0.72[d]	5	AbuTarif et al. (2014)
BCV (twice a day)	300	3.875[d]/0.944[e]	0.012[d,e]	0.0067[a,d]	0.72[d]	5	AbuTarif et al. (2014)
Triple I							
ASV (twice a day)	200	0.492	0.002	0.0063[f]	1	5	Tao et al. (2016)[g]
DCV (twice a day)	30	0.975	0.006	0.013[f]	0.71		
BCV (twice a day)	75	1.675[d]/0.350[e]	0.012[d,e]	0.0067[d,f]	0.72[d]		
Triple II							
ASV (twice a day)	200	0.473	0.002	0.0063[f]	1	5	Tao et al. (2016)[g]
DCV (twice a day)	30	0.974	0.006	0.013[f]	0.71		
BCV (twice a day)	150	3.141[d]/0.664[e]	0.012[d,e]	0.0067[d,f]	0.72[d]		

[a]Determined based on plasma concentration profile from the same study.

[b]The F_h value of ASV is calculated to be 7%, which is lower than the oral bioavailability of ASV (9.3%), suggesting ASV oral absorption is high in humans. Thus, the F_a value of ASV is set as 1.

[c]Data from an open-label, single-sequence study (AI447007), in which 18 healthy subjects (17 male and one female) received: 1) a single oral dose of 5 mg midazolam on day 1; 2) an oral dose of 600 mg ASV twice daily from day 2 to day 8; and 3) a single dose of 5 mg midazolam on day 8 (morning). The study protocol was approved by the Institutional Review Board at the investigational site (MDS Pharma Services (US) Inc., Lincoln, NE). All subjects were closely monitored for adverse events throughout the study.

[d]Values for BCV.

[e]Values for BCV-M1.

[f]Determined based on plasma concentration profile from the single agent studies.

[g]Data from an open-label, single-sequence study (AI443021), in which 20 healthy subjects (19 male and one female) received the following: 1) a cocktail of P450 and transporter probe substrates (including 5 mg midazolam) administered orally as a single dose on day 1; 2) a combination of 200 mg ASV, 20 mg DCV, and 75 mg BCV administered orally twice daily from day 6 to 20 and a cocktail of P450 and P-glycoprotein substrates (including 5 mg midazolam) administered orally as a single dose on day 16; and 3) a combination of 200 mg ASV, 20 mg DCV, and 150 mg BCV administered orally twice daily from day 21 to 35 and a cocktail of P450 and transporter probe substrates (including 5 mg midazolam) administered orally as a single dose on day 31. The study protocol was approved by the Institutional Review Board at the investigational site (IntegReview, LTD, Austin, TX). All subjects were closely monitored for adverse events throughout the study.

TABLE 5

Predictions for clinical DDI studies using basic and mechanistic static models

Perpetrator Drug	Observed AUCR (90% CI)	Predicted AUCR		
		R_3 Average[a] (Individual[b])	AUCR Average[a] (Individual[b])	AUCR'[c] Average[a] (Individual[b])
ASV (200 mg twice a day)	0.71 (0.67–0.75)	0.32 (0.26; 0.31; 0.52)	2.36 (2.29; 2.37; 2.46)	0.50 (0.35; 0.54; 0.83)
ASV (600 mg twice a day)	0.56 (0.50–0.64)	0.24 (0.18; 0.24; 0.43)	3.02 (2.94; 3.01; 3.16)	0.70 (0.51; 0.75; 1.09)
DCV (60 mg every day)	0.87 (0.83–0.92)	0.18 (0.13; 0.17; 0.32)	0.43 (0.33; 0.44; 0.68)	—[g]
BCV (150 mg twice a day)	0.50 (0.45–0.57)	0.17 (0.10; 0.26; 0.31)	0.53 (0.34; 0.70; 0.72)	—[g]
BCV (300 mg twice a day)	0.44 (0.40–0.48)	0.14 (0.08; 0.23; 0.27)	0.55 (0.34; 0.75; 0.77)	—[g]
Triple Combination I[d]	0.53 (0.47–0.60)	0.084 (0.06; 0.17)	1.94 (1.70; 2.12)	0.33 (0.21; 0.59)
Triple Combination II[e]	0.42 (0.37–0.48)	0.078 (0.05; 0.16)	1.73 (1.45; 1.94)	0.32 (0.19; 0.58)

CI, confidence interval.
[a]Model prediction using the average values of EC_{50} and E_{max} from Table 3.
[b]Model prediction using the EC_{50} and E_{max} of individual donors from Table 2.
[c]Mechanistic static model approach not including the TDI effect of ASV.
[d]ASV (200 mg twice a day); DCV (30 mg twice a day); and BCV (75 mg twice a day).
[e]ASV (200 mg twice a day); DCV (30 mg twice a day); and BCV (150 mg twice a day).
[g]Study did not involve ASV, thus AUCR' value is not applicable.

noninducer based on fold increase would be 0 and thus the calculated induction effect (eq. 9) would be 1 (no induction effect). Overall, fold increase is a more appropriate parameter for curve fitting to generate induction parameters.

The basic static model (R_3) is a simplified model used to predict in vivo DDI risk, which only considers the induction potential of the perpetrator (E_{max} and EC_{50}) at maximum plasma concentration. Therefore, the R_3 model tends to overpredict induction effects. This was apparent in our predictions from all seven clinical DDI studies, in which the R_3 values were lower in each case than the observed AUCRs. However, the R_3 model did correctly predict an induction response, defined as $R_3 < 0.9$, in these seven treatments with either single or multiple perpetrators. The mechanistic static model is a more complicated model used to evaluate the net effect of a perpetrator, which demonstrates induction, inhibition, and inactivation simultaneously in both liver and small intestine. This model also considers the characteristics of victim drugs, such as absorption and fractional metabolism through the pathway of interest. In the seven cases, the mechanistic static model was able to correctly predict the interaction risk of DCV (60 mg every day) and BCV (150 and 300 mg twice a day). Since the reversible inhibition effect was considered in this model, the predicted values are closer to the clinical observations than the R_3 values. When the TDI effect of ASV was included, the mechanistic static model incorrectly predicted the DDI risk of ASV (200 and 600 mg twice a day). This false prediction could be corrected by not including the inactivation component (B and Y in eq. 10), as shown in Table 4, which was also reported previously by Einolf et al. (2014). The detailed mechanisms for the overprediction of ASV TDI remain unclear. One explanation could be that the rapid clearance of ASV minimizes its long-lasting inactivation effect on CYP3A4, and therefore a reduced overall inhibition

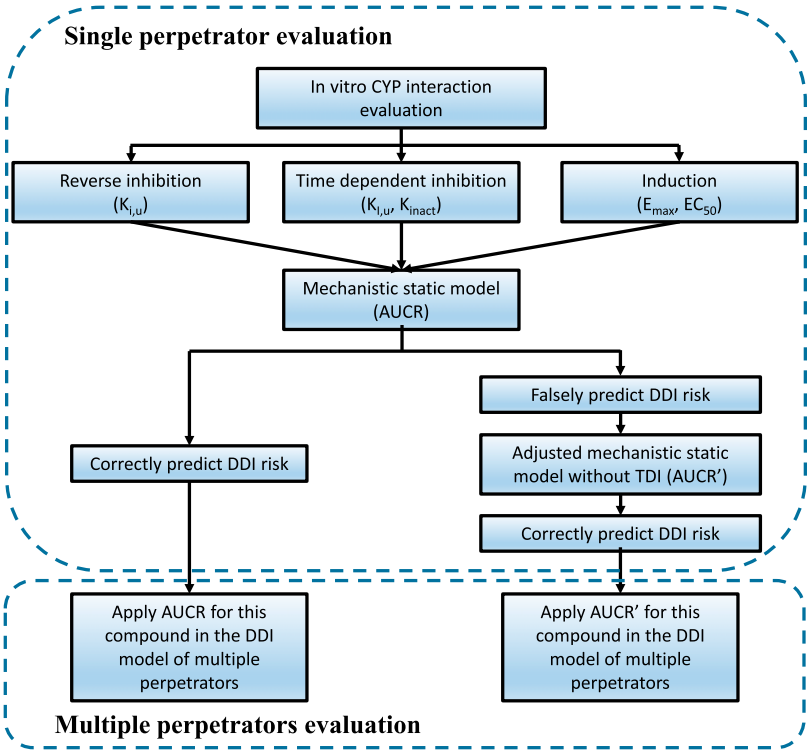

Fig. 3. Strategies to evaluate P450 DDI risk for single and multiple perpetrators using static models.

in vivo. The first-pass plasma metabolic clearance of ASV was found 49.5 l/h in the clinic (SUNVEPRA package insert). This has been observed for other high clearance drugs that demonstrated potent in vitro TDI but lower than projected clinic DDI, such as raloxifene and ezetimibe (Kosoglou et al., 2005; Parkinson et al., 2010; Zientek and Dalvie, 2012). Based on these results it seems that there is a need for better treatments of inducers that are also TDI, and the prediction of the net DDI effect of a drug that demonstrates both induction and inactivation effects should be carefully considered. In this study, we also compared the model predictions applying either average induction parameters (EC_{50} and E_{max}) or individual values. The predicted DDIs using individual parameters can potentially provide a range of ratios that could represent the individual viability in clinic. However, the small number of hepatocyte lots that are typically studied in vitro makes it very difficult to derive a meaningful projection of interindividual variability and likely does not provide useful information.

Many models have been developed to extrapolate in vitro results to in vivo observations, including static and dynamic models, in which physiologically based pharmacokinetic modeling is widely applied to predict in vivo DDIs. However, to date physiologically based pharmacokinetic approaches have been limited to prediction of DDIs with one perpetrator and it is very challenging to predict the DDI risk of mixtures of drugs using physiologically based pharmacokinetic modeling software. Here, we explored the possibility to predict DDIs with multiple inducers using static models. It has been reported that the total inhibition of multiple competitive inhibitors can be projected using the summed inhibition of each inhibitor (Venkatakrishnan et al., 2003; Lutz and Isoherranen, 2012). In this study, we assumed that the four compounds induced CYP3A4 enzymes all through the pregnane X receptor, since no CYP2B6 and CYP1A2 induction was observed in the hepatocyte experiment (data not shown). Therefore, the total induction was estimated using the summed induction of each compound, as described in eqs. 6 and 7. With these approaches, we were able to predict the net DDI risk in the presence of multiple perpetrators. Inclusion of TDI overpredicted the DDI risk for ASV alone, which then led to overprediction for two triple combination treatments including ASV. However, improved prediction was achieved for ASV when not including the TDI component. Therefore, applying the correct prediction strategy to each single perpetrator, we were able to correctly predict the DDI risk in the presence of all four perpetrators when coadministered. Based on these examples, we propose a strategy to evaluate net DDI risk with multiple perpetrators that are inducers and have a TDI component, as shown in Fig. 3. If the AUCR correctly predicts clinical DDIs for a single perpetrator, it is suggested to use the AUCR for DDI prediction of multiple perpetrators. Otherwise, prediction based on the AUCR′ should be evaluated, since our results and other literature reports have shown the overprediction when one or more of the drugs has a TDI component (Kosoglou et al., 2005; Parkinson et al., 2010; Zientek and Dalvie, 2012; Einolf et al., 2014). In the case in which the clinical DDI of each single perpetrator is unknown, we suggest calculation of both the AUCR and AUCR′ for coadministered drugs, with the use of these values according to safety and efficacy considerations of the victim drugs; prediction with the AUCR may be more appropriate with victim drugs that have safety concerns for overexposure, while prediction with the AUCR′ may be more appropriate with victim drugs that have efficacy concerns for underexposure.

While experiments using human hepatocytes have been widely accepted as the gold standard to investigate the induction effect of new chemical entities on P450 enzymes, there still remain some questions regarding exactly how to interpret induction results and translate the in vitro data into in vivo data. This is especially true for compounds that display complex inhibition and induction effects or are administered as combinations. In this study, we found that DCV, ASV, BCV, and BCV-M1 were inducers of CYP3A4 in human hepatocytes. The induction responses were fit with several models to determine kinetic parameters, and AIC_c values were used to select the best regression-fitting algorithms. The fold induction parameter was replaced by fold increase, which more accurately determined the E_{max} and EC_{50} values. This modification is especially important for compounds producing small induction effects. With model optimization and validation for single perpetrator prediction, the basic or mechanistic static model was able to predict the DDI risk for multiple perpetrators based on in vitro results.

Acknowledgments

The authors thank Xenotech, LLC, for conducting the in vitro hepatocytes induction experiments.

Authorship Contributions

Participated in research design: Cheng, Li.
Conducted experiments: Cheng, Ma, Chang, Li.
Performed data analysis: Cheng, Li.
Wrote or contributed to the writing of the manuscript: Cheng, Humphreys, Li.

References

AbuTarif M, He B, Ding Y, Sims K, Zhu K, Rege B, Pursely J, Wind-Rotolo M, Li W, and Bertz RJ (2014) The effect of steady-state BMS-791325, a non-nucleoside HCV NS5B polymerase inhibitor, on the pharmacokinetics of midazolam in healthy Japanese and Caucasian males, in *15th International Workshop on Clinical Pharmacology of HIV and Hepatitis Therapy*; 2014 May 19–21; Washington, DC. Abstract P_22.

Bifano M, Sevinsky H, Stonier M, Hao J, and Bertz RJ (2013) Daclatasvir, an HCV NS5A replication complex inhibitor, has minimal effect on pharmacokinetics of midazolam, a sensitive probe for cytochrome P450 3A4, *8th International Workshop on Clinical Pharmacology of Hepatitis Therapy*; 2013 June 26–27; Cambridge, MA. Abstract O_15.

Chang SY, Fancher RM, Zhang H, and Gan J (2010) Mechanism-based inhibition of human cytochrome P4503A4 by domperidone. *Xenobiotica* **40**:138–145.

Cheng Y and Prusoff WH (1973) Relationship between the inhibition constant (K1) and the concentration of inhibitor which causes 50 per cent inhibition (I50) of an enzymatic reaction. *Biochem Pharmacol* **22**:3099–3108.

Einolf HJ, Chen L, Fahmi OA, Gibson CR, Obach RS, Shebley M, Silva J, Sinz MW, Unadkat JD, and Zhang L, et al. (2014) Evaluation of various static and dynamic modeling methods to predict clinical CYP3A induction using in vitro CYP3A4 mRNA induction data. *Clin Pharmacol Ther* **95**:179–188.

Eley T, Gardiner DF, Persson A, He B, You X, Shah V, Sherman D, Kandoussi H, Sims KD, and Pasquinelli C, et al. (2011) Evaluation of drug interaction potential of the HCV protease inhibitor asunaprevir (ASV; BMS-650032) at 200 mg twice daily (BID) in metabolic cocktail and P-glycoprotein (P-gp) probe studies in healthy volunteers, *62th Annual Meeting of the American Association for the Study of Liver Diseases*; 2011 November 5–8; San Francisco.

Eley T, He B, Huang SP, Li W, Pasquinelli C, Rodrigues AD, Grasela DM, and Bertz RJ (2013) Pharmacokinetics of the NS3 protease inhibitor, asunaprevir (ASV, BMS-650032), in phase I studies in subjects with or without chronic hepatitis C. *Clin Pharmacol Drug Dev* **2**:316–327.

Fahmi OA, Hurst S, Plowchalk D, Cook J, Guo F, Youdim K, Dickins M, Phipps A, Darekar A, and Hyland R, et al. (2009) Comparison of different algorithms for predicting clinical drug-drug interactions, based on the use of CYP3A4 in vitro data: predictions of compounds as precipitants of interaction. *Drug Metab Dispos* **37**:1658–1666.

Fahmi OA, Maurer TS, Kish M, Cardenas E, Boldt S, and Nettleton D (2008) A combined model for predicting CYP3A4 clinical net drug-drug interaction based on CYP3A4 inhibition, inactivation, and induction determined in vitro. *Drug Metab Dispos* **36**:1698–1708.

Gao M, Nettles RE, Belema M, Snyder LB, Nguyen VN, Fridell RA, Serrano-Wu MH, Langley DR, Sun JH, and O'Boyle DR, 2nd, et al. (2010) Chemical genetics strategy identifies an HCV NS5A inhibitor with a potent clinical effect. *Nature* **465**:96–100.

Gentles RG, Ding M, Bender JA, Bergstrom CP, Grant-Young K, Hewawasam P, Hudyma T, Martin S, Nickel A, and Regueiro-Ren A, et al. (2014) Discovery and preclinical characterization of the cyclopropylindolobenzazepine BMS-791325, a potent allosteric inhibitor of the hepatitis C virus NS5B polymerase. *J Med Chem* **57**:1855–1879.

Gong J, Eley T, He B, Arora V, Philip T, Jiang H, Easter J, Humphreys WG, Iyer RA, and Li W (2016) Characterization of ADME properties of [^{14}C]asunaprevir (BMS-650032) in humans. *Xenobiotica* **46**:52–64.

Jana S and Paliwal J (2007) Molecular mechanisms of cytochrome P450 induction: potential for drug-drug interactions. *Curr Protein Pept Sci* **8**:619–628.

Kosoglou T, Statkevich P, Johnson-Levonas AO, Paolini JF, Bergman AJ, and Alton KB (2005) Ezetimibe: a review of its metabolism, pharmacokinetics and drug interactions. *Clin Pharmacokinet* **44**:467–494.

LeCluyse EL (2001) Human hepatocyte culture systems for the in vitro evaluation of cytochrome P450 expression and regulation. *Eur J Pharm Sci* **13**:343–368.

LeCluyse E, Madan A, Hamilton G, Carroll K, DeHaan R, and Parkinson A (2000) Expression and regulation of cytochrome P450 enzymes in primary cultures of human hepatocytes. *J Biochem Mol Toxicol* **14**:177–188.

Lutz JD and Isoherranen N (2012) In vitro-to-in vivo predictions of drug-drug interactions involving multiple reversible inhibitors. *Expert Opin Drug Metab Toxicol* **8**:449–466.

Madan A, Graham RA, Carroll KM, Mudra DR, Burton LA, Krueger LA, Downey AD, Czerwinski M, Forster J, and Ribadeneira MD, et al. (2003) Effects of prototypical microsomal enzyme inducers on cytochrome P450 expression in cultured human hepatocytes. *Drug Metab Dispos* **31**:421–431.

McPhee F, Sheaffer AK, Friborg J, Hernandez D, Falk P, Zhai G, Levine S, Chaniewski S, Yu F, and Barry D, et al. (2012) Preclinical profile and characterization of the hepatitis C virus NS3 protease inhibitor asunaprevir (BMS-650032). *Antimicrob Agents Chemother* **56**:5387–5396.

Obach RS, Walsky RL, and Venkatakrishnan K (2007) Mechanism-based inactivation of human cytochrome P450 enzymes and the prediction of drug-drug interactions. *Drug Metab Dispos* **35**: 246–255.

Paris BL, Ogilvie BW, Scheinkoenig JA, Ndikum-Moffor F, Gibson R, and Parkinson A (2009) In vitro inhibition and induction of human liver cytochrome P450 enzymes by milnacipran. *Drug Metab Dispos* **37**:2045–2054.

Parkinson A, Kazmi F, Buckley DB, Yerino P, Ogilvie BW, and Paris BL (2010) System-dependent outcomes during the evaluation of drug candidates as inhibitors of cytochrome P450 (CYP) and uridine diphosphate glucuronosyltransferase (UGT) enzymes: human hepatocytes versus liver microsomes versus recombinant enzymes. *Drug Metab Pharmacokinet* **25**:16–27.

Robertson P, DeCory HH, Madan A, and Parkinson A (2000) In vitro inhibition and induction of human hepatic cytochrome P450 enzymes by modafinil. *Drug Metab Dispos* **28**:664–671.

Scola PM, Sun LQ, Wang AX, Chen J, Sin N, Venables BL, Sit SY, Chen Y, Cocuzza A, and Bilder DM, et al. (2014) The discovery of asunaprevir (BMS-650032), an orally efficacious NS3 protease inhibitor for the treatment of hepatitis C virus infection. *J Med Chem* **57**: 1730–1752.

Sims KD, Lemm J, Eley T, Liu M, Berglind A, Sherman D, Lawitz E, Vutikullird AB, Tebas P, and Gao M, et al. (2014) Randomized, placebo-controlled, single-ascending-dose study of BMS-791325, a hepatitis C virus (HCV) NS5B polymerase inhibitor, in HCV genotype 1 infection. *Antimicrob Agents Chemother* **58**:3496–3503.

Sugiura N (1978) Further analysis of the data by Akaike's information criterion and the finite correction. *Commun Stat* **7**:13–26.

Tao X, Sims K, Chang YT, Rana J, Myers E, Wind-Rotolo M, Bhatnagar R, Xu T, Eley T, and Garimella T, et al. (2016) Effect of daclatasvir/asunaprevir/beclabuvir in fixed-dose combination on the pharmacokinetics of CYP450/transporter substrates in healthy subjects, *17th International Workshop on Clinical Pharmacology of HIV & Hepatitis Therapy*; 2016 June 8–10; Washington, DC. Abstract O_6.

Tompkins LM and Wallace AD (2007) Mechanisms of cytochrome P450 induction. *J Biochem Mol Toxicol* **21**:176–181.

Venkatakrishnan K, von Moltke LL, Obach RS, and Greenblatt DJ (2003) Drug metabolism and drug interactions: application and clinical value of in vitro models. *Curr Drug Metab* **4**:423–459.

Wilkins T, Malcolm JK, Raina D, and Schade RR (2010) Hepatitis C: diagnosis and treatment. *Am Fam Physician* **81**:1351–1357.

Yao M, Zhu M, Sinz MW, Zhang H, Humphreys WG, Rodrigues AD, and Dai R (2007) Development and full validation of six inhibition assays for five major cytochrome P450 enzymes in human liver microsomes using an automated 96-well microplate incubation format and LC-MS/MS analysis. *J Pharm Biomed Anal* **44**:211–223.

Zientek M and Dalvie D (2012) Use of a multistaged time-dependent inhibition assay to assess the impact of intestinal metabolism on drug-drug interaction potential. *Drug Metab Dispos* **40**: 467–473.

Address correspondence to: Dr. Wenying Li, Pharmaceutical Candidate Optimization, Bristol-Myers Squibb, P.O. Box 4000, Princeton, NJ 08543. E-mail: Wenying.Li@BMS.com